

Exact integration for the hypersingular boundary integral equation of two-dimensional elastostatics

Xiaosong Zhang[†]

*Department of Engineering Mechanics, Shijiazhuang Railway Institute,
Shijiazhuang, 050043, Hebei Province, P. R. China*

Xiaoxian Zhang[‡]

*Department of Engineering, The University of Liverpool, Brodie Tower,
Brownlow Street, Liverpool, L69 3GQ, U.K.*

(Received January 2, 2007, Accepted August 11, 2008)

Abstract. This paper presents an exact integration for the hypersingular boundary integral equation of two-dimensional elastostatics. The boundary is discretized by straight segments and the physical variables are approximated by discontinuous quadratic elements. The integral for the hypersingular boundary integral equation analysis is given in a closed form. It is proven that using the exact integration for discontinuous boundary element, the singular integral in the Cauchy Principal Value and the hypersingular integral in the Hadamard Finite Part can be obtained straightforward without special treatment. Two numerical examples are implemented to verify the correctness of the derived exact integration.

Keywords: hypersingular boundary integral equation; exact integration; singular integral in CPV; hypersingular integral in HFP.

1. Introduction

The boundary value problems can be recast into either Cauchy singular boundary integral equation or hypersingular boundary integral equation. Hong and Chen (1988) presented the theoretical bases for the dual integral equations that combined the Cauchy singular and hypersingular boundary integral equation. The hypersingular boundary integral equation has been an active area over the past few decades in various fields including degenerated boundaries (Chen *et al.* 2003), error indicator in adaptive boundary element analysis (Liang *et al.* 1999, Paulino *et al.* 2001), cracked bars under torsion (Chen *et al.* 1998), and symmetric Galerkin boundary element method (Gray *et al.* 1995). Chen *et al.* (2007) have shown the advantages of the hypersingular boundary integral equation over conventional boundary integral equation by considering free-surface seepage problems. They found that the hypersingular boundary integral equation can accelerate the rate of convergence for nonlinear surface problems. Chen and Hong (1999) gave a detailed review of

[†] Professor, Corresponding author, E-mail: xs Zhang@sjzri.edu.cn

[‡] Lecturer, E-mail: Xiaoxian.Zhang@liverpool.ac.uk

hypersingular boundary integral equation. The inherent difficulty associated with the hypersingular boundary integral equation is to effectively evaluate the singular, hypersingular and nearly singular, nearly hypersingular integrals. Tremendous effort has been expended over the past few decades to improve evaluation of these integrals (Singh and Tanaka 2001, Telles 1987, Chien 1997, Liu 1998, Luo *et al.* 1998, Chen and Liu 2001). Among the existing methods, exact integration has been proven to be efficient and accurate to estimate these integrals in different fields (Fratantonio and Rencis 2000, Yoon and Heister 2000, Mera *et al.* 2001, Friedrich 2002, Padhi *et al.* 2001, Zhang and Zhang 2003, 2004). Fratantonio and Rencis (2000) present an exact integration for two-dimensional potential problem, considering both off- and on-element integrations; they also give an exact integration to evaluate the flux at internal points. Yoon and Heister (2000) give an exact integration of linear element to compute the flux at internal points for two-dimensional potential problem using local coordinate transformation. Mera *et al.* (2001) consider the steady state anisotropic heat conduction problems using the exact integration. Friedrich (2002) presented an exact integration for linear boundary element. Zhang and Zhang (2003, 2004) derived an exact integration for the Cauchy singular boundary integral equation and present methods to evaluate the stresses of the two-dimensional elastostatics for discontinuous linear and quadratic elements; they show that the displacements and stresses at boundary points can be evaluated accurately using the exact integrations.

The discontinuous boundary element, which moves the collocation points to the interior of element, has been successful to deal with discontinuity due to geometry and boundary conditions (Xu and Brebbia 1986, Patterson and Sheikh 1989). The discontinuous boundary element has been used in BEASY commercial software (Trevelyan 1992). It is also efficient to handle the 'freedom constraint' in multi-region and FEM-BEM coupling (Zhang *et al.* 1993, Zhang and Zhang 2002). The accuracy improvement of the discontinuous boundary elements over the continuous boundary elements has been well established numerically in Mera *et al.* (2001), Florez and Power (2001) and Tadeu and Antonio (2000). Another merit of discontinuous boundary element found by the authors in (Zhang and Zhang 2004, Zhang and Zhang 2003, Zhang and Zhang 2004) is that the nearly singular, logarithmic singular integrals, singular integral in Cauchy Principal Value (CPV) and hypersingular integral in Hadamard Finite Part (HFP) can be treated in the same way as regular integrals by the exact integration, which provides an easy and efficient way to calculate the physical quantities on the boundary by the analytical integration.

The aim of this paper is to present an exact integration to evaluate the integrals in the hypersingular boundary integral equation of two-dimensional elastostatics problems with the physical quantities on the boundary approximated by discontinuous quadratic elements. It is shown that with the exact integration, the hypersingular integrals do not need special treatment and can be evaluated in the same way as the regular integrals for discontinuous elements. This greatly facilitates the computer code and improves the accuracy of boundary element analysis. The derived exact integration is validated against two numerical examples.

2. Hypersingular boundary integral equation for two-dimensional elastostatic problems

The integral representation of the interior stresses in the two-dimensional elastostatics can be written as (Brebbia 1978, Guiggiani 1995)

$$\sigma_{ij}(P) = \int_{\Gamma} D_{kij}(P, Q) u_k(Q) d\Gamma - \int_{\Gamma} S_{kij}(P, Q) t_k(Q) d\Gamma \quad (1)$$

where P is an interior point, Q is a boundary point, and S_{kij} and D_{kij} are given as follows (Brebbia 1978, Guiggiani 1995)

$$\begin{aligned} S_{kij} = \frac{k_5}{r^2} & \left\{ 2 \frac{\partial}{\partial n} [(1-2\nu) \delta_{ij} r_{,k} + \nu (\delta_{ik} r_{,j} + \delta_{jk} r_{,i}) - 4r_{,i} r_{,j} r_{,k}] \right. \\ & \left. + 2\nu (n_i r_{,j} r_{,k} + n_j r_{,i} r_{,k}) + (1-2\nu) (2n_k r_{,i} r_{,j} + n_j \delta_{ik} + n_i \delta_{jk}) - (1-4\nu) n_k \delta_{ij} \right\} \\ D_{kij} = -\frac{k_3}{r} & [(1-2\nu) (\delta_{ki} r_{,j} + \delta_{kj} r_{,i} - \delta_{ij} r_{,k}) + 2(r_i r_{,j} r_{,k})] \end{aligned} \quad (2)$$

where $k_3 = -1/4\pi(1-\nu)$ and $k_5 = G/2\pi(1-\nu)$, in which G is the shear modulus and ν is the Poisson ratio.

Taking the interior point P in Eq. (1) to the boundary as an example and considering the asymptotic analysis given in Guiggiani (1995), we have the boundary integral representation for the stresses on the boundary as follows

$$C(P) \sigma_{ij}(P) = \int_{\Gamma} D_{kij}(P, Q) u_k(Q) d\Gamma + \int_{\Gamma} S_{kij}(P, Q) t_k(Q) d\Gamma \quad (3)$$

where the free term $C(P) = 0.5$ for smooth boundary, a case for discontinuous boundary element analysis, and D_{kij} and S_{kij} are integrals existing in the Cauchy Principal Value (CPV) and the Hadamard Finite Part (HFP) respectively. The traction and stresses are related as follows (Timoshenko and Goodier 1987)

$$t_i(P) = \sigma_{ij}(P) n_j(P) \quad (4)$$

where the Einstein summation convention is used, and $n_j(P)$ ($j = 1, 2$) is the j th components of the unit outward normal at point P .

Substituting (3) into (4) gives the hypersingular boundary integral equation for the two-dimensional elastostatics:

$$C(P) t_i(P) = \int_{\Gamma} [D_{kij}(P, Q) n_j(P)] u_k(Q) d\Gamma + \int_{\Gamma} [S_{kij}(P, Q) n_j(P)] t_k(Q) d\Gamma \quad (5)$$

where $C(P) = 0.5$ for smooth boundary and $n_j(P)$ ($j = 1, 2$) is the j th components of the unit outward normal at source point P .

Eq. (5) can be recast into the following matrix form

$$\begin{aligned} C(P) \begin{Bmatrix} t_1(P) \\ t_2(P) \end{Bmatrix} &= \int_{\Gamma} \begin{bmatrix} (D_{111} n_1 + D_{112} n_2) & (D_{211} n_1 + D_{212} n_2) \\ (D_{121} n_1 + D_{122} n_2) & (D_{221} n_1 + D_{222} n_2) \end{bmatrix} \begin{Bmatrix} t_1 \\ t_2 \end{Bmatrix} d\Gamma \\ &+ \int_{\Gamma} \begin{bmatrix} (S_{111} n_1 + S_{112} n_2) & (S_{211} n_1 + S_{212} n_2) \\ (S_{121} n_1 + S_{122} n_2) & (S_{221} n_1 + S_{222} n_2) \end{bmatrix} \begin{Bmatrix} u_1 \\ u_2 \end{Bmatrix} d\Gamma \end{aligned} \quad (6)$$

Discretizing Eq. (6) gives the following algebraic equation for the hypersingular boundary integral equation

$$[H]\{u\} = [G]\{t\} \quad (7)$$

Imposing the boundary conditions, the unknown displacement and traction on the boundary can be obtained. The exact integration for the coefficient matrix $[H]$ and $[G]$ in Eq. (7) is derived in the following section.

3. Exact integration for the hypersingular boundary integral equation

The boundary is discretized into straight segments. The field points on the straight segments can be defined using the following geometric shape function:

$$x_i = \sum_{j=1}^2 N_j(\xi) x_i^j \quad (8)$$

where $N_1 = (1 - \xi)/2$ and $N_2 = (1 + \xi)/2$, (x_1^1, x_2^1) and (x_1^2, x_2^2) are the Cartesian coordinates of the two nodes of a straight segment.

The displacement and traction, which may become discontinuous at the mesh points of adjacent elements, are assumed to be quadratic

$$\begin{aligned} \begin{Bmatrix} u_1 \\ u_2 \end{Bmatrix} &= \sum_{j=1}^N [\Psi_j(\xi, \alpha) I] \begin{Bmatrix} u_1^j \\ u_2^j \end{Bmatrix} = \sum_{j=1}^N [\Psi_j(\xi, \alpha) I] \{\delta\}_j \\ \begin{Bmatrix} t_1 \\ t_2 \end{Bmatrix} &= \sum_{j=1}^N [\Psi_j(\xi, \alpha) I] \begin{Bmatrix} t_1^j \\ t_2^j \end{Bmatrix} = \sum_{j=1}^N [\Psi_j(\xi, \alpha) I] \{t\}_j \end{aligned} \quad (9)$$

where $I = \begin{bmatrix} 1 & 0 \\ 0 & 1 \end{bmatrix}$ is the unit matrix, $\{\delta\}_j$ and $\{t\}_j$ are the displacement and traction vectors respectively of the j th collocation point. In Eq. (9) the interpolation functions for the discontinuous quadratic elements are

$$\Psi_1 = \frac{1}{2} \left[\left(\frac{\xi}{\alpha} \right)^2 - \frac{\xi}{\alpha} \right], \quad \Psi_2 = 1 - \left(\frac{\xi}{\alpha} \right)^2, \quad \Psi_3 = \frac{1}{2} \left[\left(\frac{\xi}{\alpha} \right)^2 + \frac{\xi}{\alpha} \right] \quad (10)$$

where α is called collocation factor.

As shown in Fig. 1, for the collocation point P , the following geometric relationship can be obtained

$$r^2 = a\xi^2 + b\xi + c, \quad r_{,i} = \frac{C_i + D_i \xi}{r} \quad (11a)$$

$$\frac{1}{r} \frac{\partial r}{\partial n} = \frac{1}{J_0} \frac{D_2 C_1 - D_1 C_2}{a\xi^2 + b\xi + c} = \frac{1}{J_0} \frac{C_{12}}{a\xi^2 + b\xi + c} \quad (11b)$$

$$n_1 J_0 = D_2, \quad n_2 J_0 = -D_1 \quad (11c)$$

where $a = \sum_{j=1}^2 D_j^2$, $b = 2 \sum_{j=1}^2 C_j D_j$, $c = \sum_{j=1}^2 C_j^2$, $D_i = (x_i^{k+1} - x_i^k)/2$, $C_i = (x_i^{k+1} + x_i^k)/2 - x_i^P$ in which the

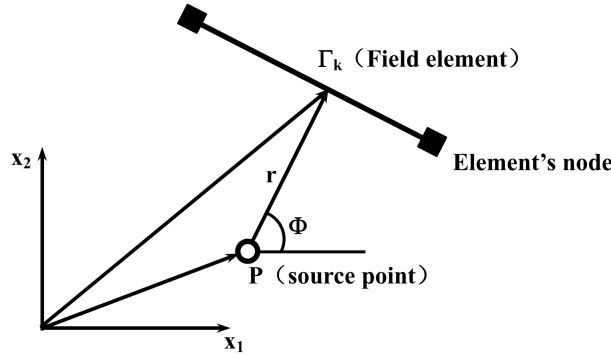


Fig. 1 Geometric relationship of the source point P and the field element Γ_k

coordinates with superscript P represent the coordinates of the source collocation point and those with superscripts k and $k + 1$ represent the coordinates of the field element's two nodes, respectively, J_0 is the Jacobian of the transformation given in Eq. (8).

To evaluate the coefficient matrix, the following integrals must be performed:

$$\int_{\Gamma} D_{kij}(P, Q)n_j(P) \Psi_S d\Gamma; \int_{\Gamma} S_{kij}(P, Q)n_j(P) \Psi_S d\Gamma \tag{12}$$

It should be noted that the term $n_j(P)$ in Eq. (12) is the unit outward normal of the source collocation point, and the integration is performed on the field elements. Thus $n_j(P)$ can be taken as a constant in the integrals.

We consider the geometric relationship for straight-segment discretization of the geometry and take $\Psi_S = \Psi_1$ as an example. The integrals in Eq. (12) can be obtained as

$$\begin{aligned} \int_{\Gamma} D_{kij}(P, Q)n_j(P) \Psi_1 d\Gamma &= \int_{-1}^{+1} D_{kij}(P, Q)n_j(P) \frac{1}{2} \frac{\xi}{\alpha} \left(\frac{\xi}{\alpha} - 1 \right) |J| d\xi \\ &= \frac{1}{2\alpha^2} \int_{-1}^{+1} D_{kij}(P, Q)n_j(P) (\xi^2 - \alpha\xi) |J| d\xi = \frac{1}{2\alpha^2} [D_{kij}^2 - \alpha D_{kij}^1] n_j(P) \\ \int_{\Gamma} S_{kij}(P, Q)n_j(P) \Psi_1 d\Gamma &= \int_{-1}^{+1} S_{kij}(P, Q)n_j(P) \frac{1}{2} \frac{\xi}{\alpha} \left(\frac{\xi}{\alpha} - 1 \right) |J| d\xi \\ &= \frac{1}{2\alpha^2} \int_{-1}^{+1} S_{kij}(P, Q)n_j(P) (\xi^2 - \alpha\xi) |J| d\xi = \frac{1}{2\alpha^2} [S_{kij}^2 - \alpha S_{kij}^1] n_j(P) \end{aligned} \tag{13}$$

where the terms D_{kij}^s and S_{kij}^s are given in the Appendix.

4. Evaluating the singular and hypersingular integrals in hypersingular boundary integral equation

The following integrals must be evaluated to analyze the hypersingular boundary integral equation

$$\int_{\Gamma_j} \frac{r_s}{r} \Psi_s d\Gamma, \int_{\Gamma_j} \frac{r_s r'_s r'_k}{r} \Psi_s d\Gamma \tag{14a}$$

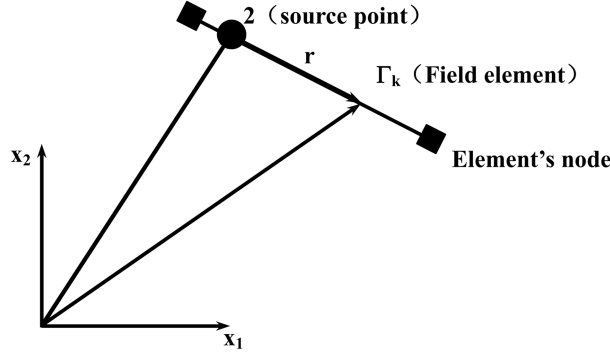


Fig. 2 Geometric relationship of the source point P on the field element Γ_k

$$\int_{\Gamma_j} \frac{1}{r^2} \Psi_s d\Gamma, \quad \int_{\Gamma_j} \frac{r_{,i} r_{,j}}{r^2} \Psi_s d\Gamma, \quad \int_{\Gamma_j} \frac{r_{,i} r_{,j} r_{,k} r_{,l}}{r^2} \Psi_s d\Gamma \tag{14b}$$

where r is the radial distance between the source and field points, $r_{,i}$ denotes the derivative of r with respect to the coordinate x_i of the field points, Ψ_s is the interpolation function given in Eq. (9).

The integrals in Eq. (14a) and Eq. (14b) exist in the CPV and HFP sense respectively for the source points on the field element. In what follows we will prove that using the exact integration for the discontinuous boundary elements, the singular and hypersingular integrals in the CPV and HFP can be evaluated in the same way as for the non-singular integrals.

We consider the case where the collocation Point 2 shown in Fig. 2 is the source point; Γ_k is the field element on which the integrals are performed. The integral is singular, and the geometric quantities in Eqs. (10), (11) for the singular integral take the following form:

$$\begin{aligned} C_1 &= -\frac{\alpha}{2}(x_1^{k+1} - x_1^k), & C_2 &= -\frac{\alpha}{2}(x_2^{k+1} - x_2^k) \\ D_1 &= \frac{1}{2}(x_1^{k+1} - x_1^k), & D_2 &= \frac{1}{2}(x_2^{k+1} - x_2^k) \\ a &= \frac{L_k^2}{4}, & b &= -\frac{\alpha L_k^2}{2}, & c &= \frac{\alpha^2 L_k^2}{4} \\ r^2 &= a\xi^2 + b\xi + c = \frac{L_k^2}{4}(\xi - \alpha)^2, & r &= \frac{L_k}{2}|\xi - \alpha| \\ r_{,1} &= \frac{D_1(\xi - \alpha)}{r}, & r_{,2} &= \frac{D_2(\xi - \alpha)}{r} \end{aligned} \tag{15}$$

where α is the collocation factor as given in Eq. (9), and L_k is the length of the straight field element.

From Eq. (15), we have the following relationship for the singular integral

$$b^2 = 4ac \tag{16}$$

The singular integral in the CPV given in Eq. (14a) can be evaluated by the exact integration (see

the Appendix for details) as follows without special treatment

$$\int_{\Gamma} \frac{r_{,1}}{r} d\Gamma = \int_{-1}^{+1} \frac{D_1(\xi - \alpha)}{(a\xi^2 + b\xi + c)} |J_0| d\xi = |J_0| D_1(F_1 - \alpha F_0)$$

$$= |J_0| D_1 \left[\frac{1}{2a} \ln \frac{a+b+c}{a-b+c} - \frac{b}{2a} F_0 - \alpha F_0 \right] = |J_0| D_1 \frac{4}{L_k^2} \ln \frac{(1-\alpha)}{(1+\alpha)}$$
(17a)

$$\int_{\Gamma} \frac{r_{,1}r_{,1}r_{,2}}{r} d\Gamma = \int_{-1}^{+1} \frac{D_1^2 D_2(\xi - \alpha)^3}{(a\xi^2 + b\xi + c)^2} |J_0| d\xi$$

$$= |J_0| D_1^2 D_2 (G_3 - 3\alpha G_2 + 3\alpha^2 G_1 - \alpha^3 G_0)$$

$$= |J_0| D_1^2 D_2 \left[\frac{16}{L_k^4} \ln \frac{(1-\alpha)}{(1+\alpha)} \right]$$
(17b)

where D_1, D_2, L_k and a, b, c are those given in Eq. (15), α is the collocation factor given in Eq. (9), F_i ($i = 0, 1$) and G_i ($i = 0, 1, 2, 3$) are given in the Appendix, and $|J_0|$ is the Jacobian determinant of the transformation from global to local coordinates as given in Eq. (8).

The hypersingular integrals in the HFP sense given in Eq. (14b) can be evaluated by the exact integration (see the Appendix for details) as follows without special treatment:

$$\int_{\Gamma} \frac{1}{r^2} d\Gamma = \int_{-1}^{+1} \frac{1}{(a\xi^2 + b\xi + c)} |J_0| d\xi = |J_0| F_0$$

$$= |J_0| \left[\frac{2}{(b-2a)} - \frac{2}{(b+2a)} \right] = -\frac{4|J_0|}{L_k^2} \left[\frac{1}{(1-\alpha)} + \frac{1}{(1+\alpha)} \right]$$
(18a)

$$\int_{\Gamma} \frac{r_{,1}r_{,2}}{r^2} d\Gamma = \int_{-1}^{+1} \frac{D_1 D_2 (\xi - \alpha)^2}{(a\xi^2 + b\xi + c)^2} |J_0| d\xi = |J_0| D_1 D_2 (G_2 - 2\alpha G_1 + \alpha^2 G_0)$$

$$= |J_0| D_1 D_2 \left[\frac{-16}{L_k^4} \left(\frac{1}{1-\alpha} + \frac{1}{1+\alpha} \right) \right]$$
(18b)

$$\int_{\Gamma} \frac{r_{,1}r_{,1}r_{,2}r_{,2}}{r^2} d\Gamma = \int_{-1}^{+1} \frac{D_1^2 D_2^2 (\xi - \alpha)^4}{(a\xi^2 + b\xi + c)^3} |J_0| d\xi$$

$$= |J_0| D_1^2 D_2^2 (K_4 - 4\alpha K_3 + 6\alpha^2 K_2 - 4\alpha^3 K_1 + \alpha^4 K_0)$$

$$= |J_0| D_1^2 D_2^2 \left[\frac{-64}{L_k^6} \left(\frac{1}{1-\alpha} + \frac{1}{1+\alpha} \right) \right]$$
(18c)

where F_0, G_i ($i = 1, 2, 3$) and K_i ($i = 1, 2, 3, 4$) are the exact integrations given in the Appendix.

It can be proven by using the Principle of Mathematical Induction that other singular and hypersingular integrals in the CPV and HFP sense of the hypersingular boundary integral equation analysis can be evaluated in the same way as in the nonsingular integral. We consider the following singular integral in the CPV sense

$$\int_{-1}^{+1} \frac{1}{\xi - \alpha} d\xi \quad (19)$$

where $\alpha \in (0, 1)$ for discontinuous boundary element. With special treatment, the singular integral in the CPV sense of Eq. (19) can be evaluated from

$$\int_{-1}^{+1} \frac{1}{\xi - \alpha} d\xi = \ln \frac{1 - \alpha}{1 + \alpha} \quad (20)$$

In the hypersingular boundary integral equation, the singular integrals in the CPV sense take the following form as shown in Eq. (1)

$$\int_{-1}^{+1} \frac{(\xi - \alpha)}{(\xi - \alpha)^2} d\xi = F_1 - \alpha F_0 = \ln \frac{1 - \alpha}{1 + \alpha} \quad (21)$$

where F_1, F_0 are given in the Appendix assuming $a = 1, b = -2\alpha, c = \alpha^2$. From Eqs. (20) and (21) we can see that the CPV of the singular integral Eq. (19) can be obtained analytically once the anti-derivative of the integrand is known. With the Principle of Mathematical Induction, it is assumed that

$$\int_{-1}^{+1} \frac{\xi^n}{\xi - \alpha} d\xi = P_n(1) - P_n(-1) \quad (22)$$

where $P_n(\xi)$ is the anti-derivative of the integrand $\xi^n/(\xi - \alpha)$, and the following relationship can be proven to be correct

$$\int_{-1}^{+1} \frac{\xi^{n+1}}{\xi - \alpha} d\xi = P_{n+1}(1) - P_{n+1}(-1) \quad (23)$$

where $P_{n+1}(\xi)$ is the anti-derivative of the integrand $\xi^{n+1}/(\xi - \alpha)$. Subtracting and adding a same term $\alpha\xi^n$ to the numerator of the integrand in Eq. (23) gives

$$\int_{-1}^{+1} \frac{\xi^{n+1} - \alpha\xi^n + \alpha\xi^n}{\xi - \alpha} d\xi = \int_{-1}^{+1} \xi^n d\xi + \int_{-1}^{+1} \frac{\alpha\xi^n}{\xi - \alpha} d\xi \quad (24)$$

It is easy to prove Eq. (23) using Eqs. (22) and (24).

In what follows we will prove that with the exact integration, the evaluation of the hypersingular integrals in HFP sense does not need special treatment.

Notice that the following hypersingular integrals in HFP sense can be obtained with the special treatment as follows

$$\int_{-1}^{+1} \frac{1}{(\xi - \alpha)^2} d\xi = \frac{1}{1 + \alpha} - \frac{1}{1 - \alpha} \quad (25)$$

Similarly as in Eq. (19), the hypersingular integrals in the HFP sense of Eq. (25) can be evaluated using the exact integration for discontinuous boundary elements without special treatment. Therefore, the HFP of the hypersingular integrals given in Eq. (25) can be obtained analytically once the anti-derivative of the integrand is known.

With the Principle of Mathematical Induction, it is assumed that the following formula is true

$$\int_{-1}^{+1} \frac{\xi^n}{(\xi - \alpha)^2} d\xi = S_n(1) - S_n(-1) \quad (26)$$

where $S_n(\xi)$ is the anti-derivative of the integrand $\xi^n/(\xi-\alpha)^2$. It can prove that the following relationship is true

$$\int_{-1}^{+1} \frac{\xi^{n+1}}{(\xi-\alpha)^2} d\xi = S_{n+1}(1) - S_{n+1}(-1) \quad (27)$$

where $S_{n+1}(\xi)$ is the anti-derivative of the integrand $\xi^{n+1}/(\xi-\alpha)^2$. Subtracting and adding a same term $\alpha\xi^n$ to the numerator of the integrand in Eq. (27) gives

$$\int_{-1}^{+1} \frac{\xi^{n+1} - \alpha\xi^n + \alpha\xi^n}{(\xi-\alpha)^2} d\xi = \int_{-1}^{+1} \frac{\xi^n}{\xi-\alpha} d\xi + \int_{-1}^{+1} \frac{\alpha\xi^n}{(\xi-\alpha)^2} d\xi \quad (28)$$

From Eqs. (26) and (28), it is easy to prove Eq. (27).

5. Numerical examples

Two examples are implemented to verify the derived exact integration. The first example is a parallelogram plate under linear displacement, and the second example is the shear lag analysis of a rectangle plate under shear loading.

5.1 Parallelogram plate under linear displacement

This is a benchmark problem and Fig. 3 shows the geometry. The displacement field derived and applied to a patch test of FEM-BEM coupling procedure in Lu *et al.* (1991) is given as follows

$$\begin{aligned} u_1 &= \frac{1}{5}(x_1 + x_2) \times 10^{-2} \\ u_2 &= \frac{1}{2}(x_1 + x_2) \times 10^{-3} \end{aligned} \quad (29)$$

The plate is assumed to be in the state of plane stress condition. The mechanical properties of the material are: the elastic modulus $E = 211 \times 10^9$ Pa and Poisson ratio $\nu = 0.3$. The stresses associated with the displacement can be obtained from the strain-displacement relationship and the constitutive equation as follows

$$\begin{Bmatrix} \sigma_x \\ \sigma_y \\ \sigma_{xy} \end{Bmatrix} = \frac{E}{(1-\nu^2)} \begin{bmatrix} 1 & \nu & 0 \\ \nu & 1 & 0 \\ 0 & 0 & \frac{1-\nu}{2} \end{bmatrix} \begin{Bmatrix} \varepsilon_x \\ \varepsilon_y \\ \gamma_{xy} \end{Bmatrix} = \begin{Bmatrix} 0.4985164836 \\ 0.2550549451 \\ 0.2028846154 \end{Bmatrix} \times 10^9 (Pa) \quad (30)$$

The problem is solved with the integrals being estimated using the derived exact integration. Four discontinuous quadratic elements are used to discretize the boundary, and the collocation factor in the discontinuous linear element is taken as $\alpha = 0.5$. The boundary conditions at the collocation points are prescribed displacements, which are calculated from Eq. (29). The coordinates of the point C shown in Fig. 2 are (4, 6). The coefficients of the matrix $[H]$ and $[G]$ for the hypersingular and Cauchy singular boundary integral equations are given in Table 1 and Table 2, respectively.

Table 1 The coefficients of the matrix [H] and [G] in the hypersingular boundary integral equation ($E = 211 \times 10^9$ Pa, $\nu = 0.3$ and $\alpha = 0.5$)

H ₇₁	H ₇₂	H ₇₇	H ₇₈	H ₇₉	G ₇₁	G ₇₂	G ₇₇	G ₇₈	G ₇₉
0.35843E+10	-0.16852E+08	-0.13181E+11	0.52555E+02	-0.24216E+11	-0.74844E-01	0.14937E-01	-0.50000E+00	0.16162E+00	0.83267E-16

Table 2 The coefficients of the matrix [H] and [G] in the Cauchy singular boundary integral equation ($E = 211 \times 10^9$ Pa, $\nu = 0.3$, $\alpha = 0.5$)

H ₇₁	H ₇₂	H ₇₇	H ₇₈	H ₇₉	G ₇₁	G ₇₂	G ₇₇	G ₇₈	G ₇₉
-0.58193E-01	0.10139E-01	0.50000E+00	0.16162E+00	0.00000E+00	-0.18635E-11	0.39143E-12	0.26456E-11	0.10198E-11	0.15808E-11

Table 3 Comparison of the stresses at internal point calculated using the Cauchy singular boundary integral equation (CBIE) and the hypersingular boundary integral equation (HBIE) ($\alpha = 0.5$)

Coordinates		(4.025,2.0)	(2.025,2)	(3.025,2.0)
CBIE	σ_x	0.49850980E+09	0.49851005E+09	0.49850996E+09
	σ_y	0.25505309E+09	0.25505284E+09	0.25505228E+09
	τ_{xy}	0.20288364E+09	0.20288387E+09	0.20288326E+09
HBIE	σ_x	0.49851646E+09	0.49851646E+09	0.49851646E+09
	σ_y	0.25505493E+09	0.25505493E+09	0.25505493E+09
	τ_{xy}	0.20288461E+09	0.20288461E+09	0.20288461E+09
Exact	σ_x		0.4985164836E+09	
	σ_y		0.255054951E+09	
	τ_{xy}		0.2028846154E+09	

In both the Cauchy singular and hypersingular boundary integral equations, the traction along the boundary can be obtained from Eq. (7) by enforcing the prescribed displacement boundary condition calculated by Eq. (29). The stresses in interior points can be obtained using Eq. (1) assuming $C(P) = 1$ with the obtained traction and the prescribed displacement boundary condition. The stresses evaluated at several internal points by the hypersingular and Cauchy singular boundary integral equations are given in Table 3. Comparing with the analytical values given in Eq. (31), the results obtained by the hypersingular boundary integral equation and Cauchy singular boundary integral equations are both in high precision. The hypersingular boundary integral equation is accurate to the 7th decimal, while the Cauchy singular boundary integral equation is accurate to 5th decimal. This might be due to the improvement of condition number of matrix in hypersingular boundary integral equation as given in Chen *et al.* (2007).

We change the coordinates of the Point C (x_3, y_3) shown in Fig. 3 to verify the correctness of the exact integration for arbitrary quadrilateral. The displacements calculated from Eq. (29) are used as prescribed displacement boundary condition, and the results (not presented) also show good agreement with the exact solution.

5.2 Shear lag of plate under varying shear load

The shear lag phenomenon is intensively studied for box girder. A rectangle plate in plane stress

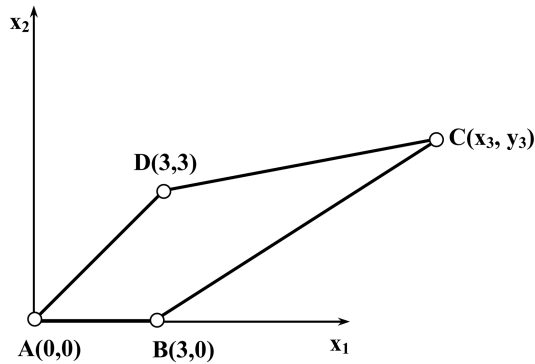


Fig. 3 Quadrilateral domain under prescribed displacement boundary condition

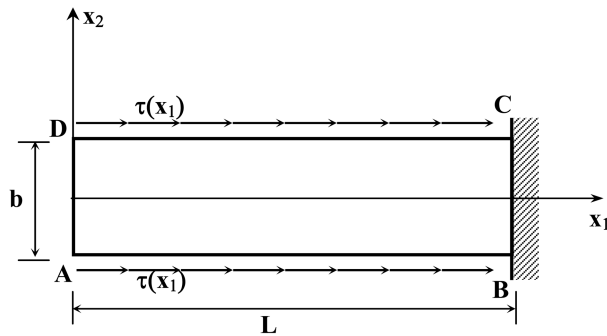


Fig. 4 The rectangle plate under shear loading along the boundary for shear lag analysis

state is taken as a model to gain physical insight into the shear lag effect. A rectangle under distributed shear loading shown in Fig. 4 is taken as an example for the shear lag analysis. The distributed shear loading on AB and CD varies according to

$$\tau(x) = \frac{(n + 1) \tau_0}{2} \left(\frac{x_1}{L}\right)^n \tag{31}$$

The resulting shear loading given in Eq. (31) can be obtained as

$$T = \int_0^L \tau(x) dx = \frac{\tau_0 L}{2} \tag{32}$$

Eq. (32) shows that the shear loading is independent of n , the order of the polynomial of the distributed shear load. From the elementary theory of the mechanics of material of axially loaded member, we can be obtained the unit normal stress on BC as

$$\sigma = \frac{\tau_0 L}{b} \tag{33}$$

The hypersingular boundary integral equation with the integrals evaluated using the exact integration is used to analyze the problem shown in Fig. 4 under the shear loading given Eq. (31) for different n . The elastic modulus is $E = 211 \times 10^9$ Pa and the Poisson ratio is $\nu = 0.3$. The collocation factor is taken as $\alpha = 0.5$. The length of the plate is $L = 10$ m, the width is $b = 3$ m, and

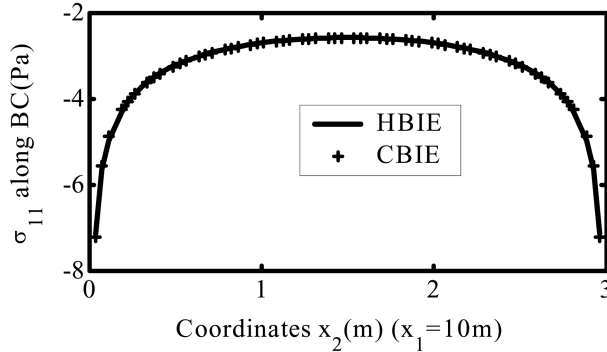


Fig. 5 The calculated unit normal stress σ_{11} along the boundary BC shown Fig. 1 using HBIE and CBIE

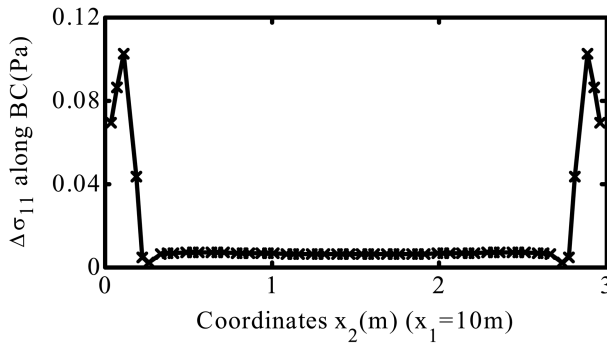


Fig. 6 The absolute error of the unit normal stress σ_{11} along the boundary BC shown in Fig. 1 given by the HBIE and CBIE

the problem is assumed to be in the state of plane stress.

The boundary is discretized with 80 discontinuous quadratic elements with each side having 20 elements. To verify the correctness of the exact integration, the Cauchy singular and the hypersingular boundary integral equations are used to analyze the problem with $n = 1$. Fig. 5 shows the unit normal stress along BC calculated by the two methods, and Fig. 6 gives the error defined as

$$\Delta\sigma_{11} = |\sigma^{HBIE} - \sigma^{CBIE}| \tag{34}$$

where the quantity with superscript HBIE represents the results obtained by the hypersingular boundary integral equation, and that with CBIE denotes the results obtained from the Cauchy singular boundary integral equation. Fig. 5 shows that results obtained by the HBIE and CBIE are in good agreement. Fig. 6 gives the absolute error by CBIE and HBIE. Large oscillation can be found in the vicinity of points B and C. This is due to the high stress gradient near the two ends of the boundary, which is also observed in Zhang and Zhang (2004) for Cook problem analysis. It lays the foundation for adaptive boundary element analysis (Liang *et al.* 1999, Paulino *et al.* 2001).

The unit normal stress σ_{11} along BC calculated using different n is shown in Fig. 7. It can be seen that the shear lag effect becomes pronounced with the increase of n . The unit normal stress σ_{11} along BC obtained with different mesh discretization are also considered and Fig. 8 compares the results obtained with 80 and 160 discontinuous quadratic elements for loading $n = 100$ in Eq. (31). They are in good agreement.

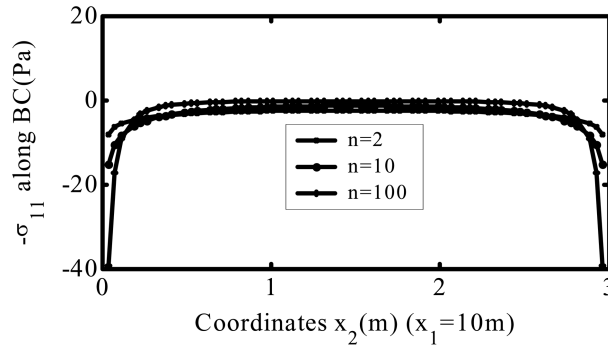


Fig. 7 The unit normal stress σ_{11} distribution along the boundary BC shown Fig. 1 under different loading conditions

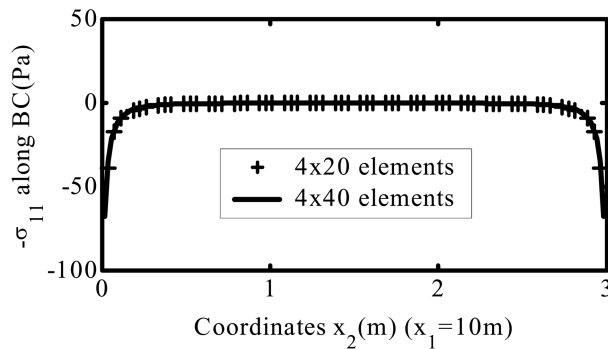


Fig. 8 The calculated unit normal stress σ_{11} distribution along the boundary BC shown in Fig. 1 under loading condition ($n = 100$ in Eq. (31)) using different discretizations

6. Conclusions

In this paper, the hypersingular boundary integral equation is derived based on the integral representation of boundary stresses. The boundary is discretized by the straight segment, and the physical variables are approximated by discontinuous quadratic interpolation function. The exact integration of the hypersingular boundary integral equation analysis is derived in a closed form. It is proven that the singular and the hypersingular integrals in the CPV and HFP can be accurately calculated using the exact integration without special treatments; this greatly simplifies computer code. Two examples are implemented to prove the correctness of the exact integration.

Acknowledgements

We are grateful to the anonymous reviewers for their insightful and constructive comments and suggestions to improve the manuscript.

References

- Brebbia, C.A. (1978), *The Boundary Element Method for Engineers*. Pentech Press, London.
- Brebbia, C.A. and Dominguez, J. (1989), *Boundary Elements: An Introductory Course*. Computational Mechanics Publications; Southampton.
- Chen, J.T. and Hong, H.K. (1992), *Boundary Element Methods*, 2nd Edition, New World Press, Taipei.
- Chen, J.T. and Hong, H.K. (1999), "Review of dual boundary element methods with emphasis on hypersingular integrals and divergent series", *Appl. Mech. Review*, **52**(1), 17-33.
- Chen, J.T., Chen, K.H., Yeh, W. and Shieh, N.C. (1998), "Dual boundary element analysis for cracked bars under torsion", *Eng. Comput.*, **15**, 732-749.
- Chen, J.T., Hsiao, C.C., Chiu, P.Y. and Lee, Y.T. (2007), "Study of free-surface seepage problems using hypersingular equations", *Comm. Numer. Meth. Eng.*, DOI:10.1002/cnm.925 (in Press).
- Chen, J.T., Kuo, S.R. and Lin, J.H. (2003), "Analytical study and numerical experiments for degenerate scale problems in boundary element method for two-dimensional elasticity", *Int. J. Numer. Meth. Eng.*, **54**, 1669-1681.
- Chen, X.L. and Liu, Y.J. (2001), "Thermal stress analysis of multi-layer thin film and coatings by an advanced boundary element method", *CMES: Comput. Modeling Eng. Sci.*, **2**(3), 337-349.
- Chien, C.C., You, Z.Y. and Chung, Y.L. (1997), "Internal stress calculation using an iterative subdivision scheme in the boundary element method", *Eng. Anal. Bound. Elem.*, **20**, 145-153.
- Florez, W.F. and Power, H. (2001), "Comparison between continuous and discontinuous boundary elements in multidomain dual reciprocity method for the solution of two-dimensional Navier-Stokes equations", *Eng. Anal. Bound. Elem.*, **25**, 57-69.
- Fratantonio, M. and Rencis, J.J. (2000), "Exact boundary element integrations for two-dimensional Laplace equation", *Eng. Anal. Bound. Elem.*, **24**, 325-342.
- Friedrich, F. (2002), "A linear analytical boundary element method for 2D homogeneous potential problems", *Comput. Geosci.*, **28**(5), 679-692.
- Gray, L.J., Chinta, B. and Kane, J.H. (1995), "Symmetric Galerkin fracture analysis", *Eng. Anal. Bound. Elem.*, **15**, 103-109.
- Guiggiani, M. (1995), "Hypersingular boundary integral equations have an additional term", *Comput. Mech.*, **16**, 245-248.
- Hong, H.K. and Chen, J.T. (1988), "Derivation of integral equations of Elasticity", *J. Eng. Mech.*, **114**(6), 1028-1044.
- Liang, M.T., Chen, J.T. and Yang, S.S. (1999), "Error estimation for boundary element method", *Eng. Anal. Bound. Elem.*, **23**, 257-265.
- Liu, Y.J. (1998), "Analysis of shell-like structures by boundary element method based on 3-D elasticity: Formulation and verification", *Int. J. Numer. Meth. Eng.*, **41**, 541-558.
- Lu, Y.Y., Belytschko, T. and Liu, W.K. (1991), "A variationally coupled FE-BE method for elasticity and fracture mechanics", *Comput. Meth. Appl. Mech. Eng.*, **85**, 21-37.
- Luo, J.F., Liu, Y.J. and Berger, E.J. (1998), "Analysis of two-dimensional thin structures (from micro- to nano-scales) using the boundary element method", *Comput. Mech.*, **22**, 404-412.
- Mera, N.S., Elliott, L., Ingham, D.B. and Lesnic, D. (2001), "A comparison of boundary element method formulations for anisotropic heat conduction problems", *Eng. Anal. Bound. Elem.*, **25**, 115-128.
- Padhi, G.S., Shenoi, R.A., Moy, S.S.J. and McCarthy, M.A. (2001), "Analytic integration of kernel shape function product integrals in boundary element method", *Comput. Struct.*, **79**, 1325-1333.
- Patterson, C. and Sheikh, M.A. (1989), "Interelement continuity in boundary element method", In *Topics in Boundary Element Research*. Springer-Verlag, **1**, 123-141.
- Paulino, G.H., Menon, G. and Mukherjee, S. (2001), "Error estimation using hypersingular integrals in boundary element methods for linear elasticity", *Eng. Anal. Bound. Elem.*, **25**, 523-534.
- Singh, K.M. and Tanaka, M. (2001), "On non-linear transformation for accurate numerical evaluation of weakly singular boundary integrals", *Int. J. Numer. Meth. Eng.*, **50**, 2007-2030.
- Tadeu, A. and Antonio, J. (2000), "Use of constant, linear and quadratic boundary elements in 3D wave diffraction analysis", *Eng. Anal. Bound. Elem.*, **25**, 131-144.

- Telles, J.C.F. (1987), "A self-adaptive co-ordinate transformation for efficient numerical evaluation of general boundary integrals", *Int. J. Numer. Meth. Eng.*, **24**, 959-973.
- Timoshenko, S.P. and Goodier, J.N. (1987), *Theory of Elasticity*. 3rd edition. McGraw-Hill, New York.
- Trevelyan, J. (1992), "Use of discontinuous boundary elements for fracture mechanics analysis", *Eng. Anal. Bound. Elem.*, **10**, 353-358
- Xu, J.M. and Brebbia, C.A. (1986), "Optimum positions for nodes in discontinuous boundary element", *Proceeding of 8th International Conference on BEM*, Springer-Verlag, 761-767.
- Yoon, S.S. and Heister, S.D. (2000), "Analytic solution for fluxes at interior points for 2D Laplace equation", *Eng. Anal. Bound. Elem.*, **24**, 155-160.
- Zhang, X.S. and Zhang X.X. (2004), "Exact integrations of two-dimensional high-order discontinuous boundary elements of elastostatics problems", *Eng. Anal. Bound. Elem.*, **28**, 725-732.
- Zhang, X.S. and Zhang, X.X. (2002), "Coupling FEM and discontinuous BEM for elastostatics and fluid-structure interaction", *Eng. Anal. Bound. Elem.*, **26**, 719-725.
- Zhang, X.S. and Zhang, X.X. (2003), "Exact integration in the boundary element method for two-dimensional elastostatics problems", *Eng. Anal. Bound. Elem.*, **27**, 987-997.
- Zhang, X.S. and Zhang, X.X. (2004), "Exact integration for stress evaluation in boundary element analysis of two-dimensional elastostatics", *Eng. Anal. Bound. Elem.*, **28**, 997-1004.
- Zhang, X.S., Ye, T.Q. and Wang, R.P. (1993), "Multi-domain boundary element method and its parallelization", In *Boundary Element Method*, Elsevier Science Publishers, 67-78.

Appendix

$$S_{111}^i = k_5 \{ 2C_{12}[(C_1G_i + D_1G_{i+1}) - 4(C_1^3K_i + 3C_1D_1K_{i+1} + 3C_1D_1^2K_{i+2} + D_1^3K_{i+3})] \\ + 2D_2(C_1^2G_i + 2C_1D_1G_{i+1} + D_1^2G_{i+2}) + D_2F_i \} \quad (A1)$$

$$S_{211}^i = k_5 \{ 2C_{12}[(1-2\nu)(C_2G_i + D_2G_{i+1}) - 4(C_1^2C_2K_i + (C_1^2D_2 + 2C_1C_2D_1)K_{i+1} + (2C_1D_1D_2 + C_2D_1^2)K_{i+2} + D_1^2D_2K_{i+3})] \\ + 4\nu D_2(C_1C_2G_i + (C_1D_2 + C_2D_1)G_{i+1} + D_1D_2G_{i+2}) - 2(1-2\nu)D_1(C_1^2G_i + 2C_1D_1G_{i+1} + D_1^2G_{i+2}) + (1-4\nu)D_1F_i \} \quad (A2)$$

$$S_{122}^i = k_5 \{ 2C_{12}[(1-2\nu)(C_1G_i + D_1G_{i+1}) - 4(C_1C_2^2K_i + (C_2^2D_1 + 2C_1C_2D_2)K_{i+1} + (2C_2D_1D_2 + C_1D_2^2)K_{i+2} + D_1D_2^2K_{i+3})] \\ - 4\nu D_1(C_1C_2G_i + (C_1D_2 + C_2D_1)G_{i+1} + D_1D_2G_{i+2}) + 2(1-2\nu)D_2(C_2^2G_i + 2C_2D_2G_{i+1} + D_2^2G_{i+2}) - (1-4\nu)D_2F_i \} \quad (A3)$$

$$S_{222}^i = k_5 \{ 2C_{12}[(C_2G_i + D_2G_{i+1}) - 4(C_2^3K_i + 3C_2^2D_2K_{i+1} + 3C_2D_2^2K_{i+2} + D_2^3K_{i+3})] \\ - 2D_1(C_2^2G_i + 2C_2D_2G_{i+1} + D_2^2G_{i+2}) - D_1F_i \} \quad (A4)$$

$$S_{112}^i = k_5 \{ 2C_{12} \{ \nu(C_2G_i + D_2G_{i+1}) - 4[C_1^2C_2K_i + (C_1^2D_2 + 2C_1C_2D_1)K_{i+1} + (2C_1D_1D_2 + C_2D_1^2)K_{i+2} + D_1^2D_2K_{i+3}] \} \\ - 2\nu D_1(C_1^2G_i + 2C_1D_1G_{i+1} + D_1^2G_{i+2}) + 2(1-\nu)D_2(C_1C_2G_i + (C_1D_2 + C_2D_1)G_{i+1} + D_1D_2G_{i+2}) - (1-2\nu)D_1F_i \} \quad (A5)$$

$$S_{212}^i = k_5 \{ 2C_{12}[\nu(C_1G_i + D_1G_{i+1}) - 4[C_1C_2^2K_i + (C_2^2D_1 + 2C_1C_2D_2)K_{i+1} + (C_1D_2^2 + 2C_2D_1D_2)K_{i+2} + D_1D_2^2K_{i+3}] \\ + 2\nu D_2(C_2^2G_i + 2C_2D_2G_{i+1} + D_2^2G_{i+2}) - 2(1-\nu)D_1(C_1C_2G_i + (C_1D_2 + C_2D_1)G_{i+1} + D_1D_2G_{i+2}) + (1-2\nu)D_2F_i \} \quad (A6)$$

$$D_{111}^i = -k_3J_0[(1-2\nu)(C_1F_i + D_1F_{i+1}) + 2(C_1^3G_i + 3C_1^2D_1G_{i+1} + 3C_1D_1^2G_{i+2} + D_1^3G_{i+3})] \quad (A7)$$

$$D_{211}^i = -k_3J_0\{-(1-2\nu)(C_2F_i + D_2F_{i+1}) + 2[C_1^2C_2G_i + (C_1^2D_2 + 2C_1C_2D_1)G_{i+1} + (2C_1D_1D_2 + C_2D_1^2)G_{i+2} + D_1^2D_2G_{i+3}]\} \quad (A8)$$

$$D_{122}^i = -k_3J_0\{-(1-2\nu)(C_1F_i + D_1F_{i+1}) + 2[C_1C_2^2G_i + (C_2^2D_1 + 2C_1C_2D_2)G_{i+1} + (2C_2D_1D_2 + C_1D_2^2)G_{i+2} + D_1D_2^2G_{i+3}]\} \quad (A9)$$

$$D_{222}^i = -k_3J_0[(1-2\nu)(C_2F_i + D_2F_{i+1}) + 2(C_2^3G_i + 3C_2^2D_2G_{i+1} + 3C_2D_2^2G_{i+2} + D_2^3G_{i+3})] \quad (A10)$$

$$D_{112}^i = -k_3J_0\{-(1-2\nu)(C_2F_i + D_2F_{i+1}) + 2[C_1^2C_2G_i + (C_1^2D_2 + 2C_1C_2D_1)G_{i+1} + (2C_1D_1D_2 + C_2D_1^2)G_{i+2} + D_1^2D_2G_{i+3}]\} \quad (A11)$$

$$D_{212}^i = -k_3J_0\{-(1-2\nu)(C_1F_i + D_1F_{i+1}) + 2[C_1C_2^2G_i + (C_2^2D_1 + 2C_1C_2D_2)G_{i+1} + (2C_2D_1D_2 + C_1D_2^2)G_{i+2} + D_1D_2^2G_{i+3}]\} \quad (A12)$$

In Eqs. (A1)-(A12), k_3 and k_5 are given in Eq. (3), and C_i , D_i ($i = 1, 2$) are given in Eqs. (9)-(12), J_0 is the Jacobian of the transformation given in Eq. (4), F_i ($i = 1\sim 6$), G_i ($i = 1\sim 6$) and K_i ($i = 1\sim 6$) are given as follows

$$F_i = \int_{-1}^{+1} \frac{x^i}{(ax^2 + bx + c)} dx \quad (A13)$$

$$G_i = \int_{-1}^{+1} \frac{x^i}{(ax^2 + bx + c)^2} dx \quad (A14)$$

$$K_i = \int_{-1}^{+1} \frac{x^i}{(ax^2 + bx + c)^3} dx \tag{A15}$$

where a, b, c and $C_i, D_i (i = 1, 2)$ are those given in Eqs. (9)-(12), and $F_i (i = 1\sim 6), G_i (i = 1\sim 6)$ and $K_i (i = 1\sim 6)$ can be obtained explicitly as follows

$$F_0 = \begin{cases} \frac{2}{\sqrt{4ac-b^2}} \left(\arctan \frac{2a+b}{\sqrt{4ac-b^2}} - \arctan \frac{-2a+b}{\sqrt{4ac-b^2}} \right) & (4ac > b^2) \\ \frac{2}{b-2a} - \frac{2}{b+2a} & (4ac = b^2) \end{cases} \tag{A16}$$

$$F_1 = \frac{1}{2a} \ln \frac{a+b+c}{a-b+c} - \frac{b}{2a} F_0 \tag{A17}$$

$$F_2 = \frac{2}{a} - \frac{c}{a} F_0 - \frac{b}{a} F_1 \tag{A18}$$

$$F_3 = -\frac{c}{a} F_1 - \frac{b}{a} F_2 \tag{A19}$$

$$F_4 = \frac{2}{3a} - \frac{c}{a} F_2 - \frac{b}{a} F_3 \tag{A20}$$

$$F_5 = -\frac{c}{a} F_3 - \frac{b}{a} F_4 \tag{A21}$$

$$F_6 = \frac{2}{5a} - \frac{c}{a} F_4 - \frac{b}{a} F_5 \tag{A22}$$

$$G_0 = \begin{cases} \frac{(2a+b)}{(4ac-b^2)(a+b+c)} - \frac{(-2a+b)}{(4ac-b^2)(a-b+c)} + \frac{2a}{(4ac-b^2)} F_0 & (b^2 \neq 4ac) \\ \frac{8a}{3(b-2a)^3} - \frac{8a}{3(b+2a)^3} & (b^2 = 4ac) \end{cases} \tag{A23}$$

$$G_1 = \begin{cases} \frac{(b+2c)}{(b^2-4ac)(a+b+c)} - \frac{-b+2c}{(b^2-4ac)(a-b+c)} + \frac{b}{(b^2-4ac)} F_0 & (b^2 \neq 4ac) \\ -\left(\frac{8a}{3(2a+b)^3} + \frac{8a}{3(-2a+b)^3} \right) - \frac{2}{3} \left(\frac{1}{(2a+b)^2} - \frac{1}{(-2a+b)^2} \right) & (b^2 = 4ac) \end{cases} \tag{A24}$$

$$G_2 = \frac{-1}{a(a-b+c)} - \frac{1}{a(a+b+c)} + \frac{c}{a} G_0 \tag{A25}$$

$$G_3 = \frac{1}{2a^2} \left(\ln \frac{a+b+c}{a-b+c} - 3abG_2 - (2ac+b^2)G_1 - bcG_0 \right) \tag{A26}$$

$$G_4 = \frac{1}{a} \left(\frac{1}{a+b+c} + \frac{1}{a-b+c} \right) - \frac{2b}{a} G_3 - \frac{3c}{a} G_2 \tag{A27}$$

$$G_5 = \frac{1}{2a} \left(\frac{1}{a+b+c} - \frac{1}{a-b+c} \right) - \frac{3b}{2a} G_4 - \frac{2c}{a} G_3 \tag{A28}$$

$$G_6 = \frac{1}{3a} \left(\frac{1}{a+b+c} + \frac{1}{a-b+c} \right) - \frac{4b}{3a} G_5 \quad (\text{A29})$$

$$K_0 = \begin{cases} -\frac{32a^2}{5} \left[\frac{1}{(2a+b)^5} - \frac{1}{(-2a+b)^5} \right] & (b^2 = 4ac) \\ \frac{1}{2(4ac-b^2)} \left[\frac{b+2a}{(a+b+c)^2} - \frac{b-2a}{(a-b+c)^2} \right] + \frac{6a}{2(4ac-b^2)} G_0 & (b^2 \neq 4ac) \end{cases} \quad (\text{A30})$$

$$K_1 = \begin{cases} -\frac{32a^2}{5} \left[\frac{1}{(2a+b)^5} + \frac{1}{(-2a+b)^5} \right] - \frac{4a}{5} \left[\frac{1}{(2a+b)^4} - \frac{1}{(-2a+b)^4} \right] & (b^2 = 4ac) \\ \frac{-1}{2(4ac-b^2)} \left[\frac{b+2c}{(a+b+c)^2} + \frac{b-2c}{(a-b+c)^2} \right] + \frac{-3b}{2(4ac-b^2)} G_0 & (b^2 \neq 4ac) \end{cases} \quad (\text{A31})$$

$$K_2 = -\frac{1}{3a} \left[\frac{1}{(a+b+c)^2} + \frac{1}{(a-b+c)^2} \right] - \frac{b}{3a} K_1 + \frac{c}{3a} K_0 \quad (\text{A32})$$

$$K_3 = -\frac{1}{2a} \left[\frac{1}{(a+b+c)^2} - \frac{1}{(a-b+c)^2} \right] + \frac{c}{a} K_1 \quad (\text{A33})$$

$$K_4 = -\frac{1}{a} \left[\frac{1}{(a+b+c)^2} + \frac{1}{(a-b+c)^2} \right] + \frac{b}{a} K_3 + \frac{3c}{a} K_2 \quad (\text{A34})$$

$$K_5 = \frac{1}{a} G_5 - \frac{b}{a} K_4 - \frac{c}{a} K_3 \quad (\text{A35})$$

$$K_6 = \frac{1}{a} \left[\frac{1}{(a+b+c)} + \frac{1}{(a-b+c)} \right] - \frac{3b}{a} K_5 - \frac{5c}{a} K_4 \quad (\text{A36})$$